NASA/TM—2003-212589 AIAA–2003–4865

Characterization of Downstream Ion Energy Distributions From a High Current Hollow Cathode in a Ring Cusp Discharge Chamber

John E. Foster and Michael J. Patterson
Glenn Research Center, Cleveland, Ohio

October 2003

The NASA STI Program Office . . . in Profile

Since its founding, NASA has been dedicated to the advancement of aeronautics and space science. The NASA Scientific and Technical Information (STI) Program Office plays a key part in helping NASA maintain this important role.

The NASA STI Program Office is operated by Langley Research Center, the Lead Center for NASA's scientific and technical information. The NASA STI Program Office provides access to the NASA STI Database, the largest collection of aeronautical and space science STI in the world. The Program Office is also NASA's institutional mechanism for disseminating the results of its research and development activities. These results are published by NASA in the NASA STI Report Series, which includes the following report types:

- TECHNICAL PUBLICATION. Reports of completed research or a major significant phase of research that present the results of NASA programs and include extensive data or theoretical analysis. Includes compilations of significant scientific and technical data and information deemed to be of continuing reference value. NASA's counterpart of peer-reviewed formal professional papers but has less stringent limitations on manuscript length and extent of graphic presentations.

- TECHNICAL MEMORANDUM. Scientific and technical findings that are preliminary or of specialized interest, e.g., quick release reports, working papers, and bibliographies that contain minimal annotation. Does not contain extensive analysis.

- CONTRACTOR REPORT. Scientific and technical findings by NASA-sponsored contractors and grantees.

- CONFERENCE PUBLICATION. Collected papers from scientific and technical conferences, symposia, seminars, or other meetings sponsored or cosponsored by NASA.

- SPECIAL PUBLICATION. Scientific, technical, or historical information from NASA programs, projects, and missions, often concerned with subjects having substantial public interest.

- TECHNICAL TRANSLATION. English-language translations of foreign scientific and technical material pertinent to NASA's mission.

Specialized services that complement the STI Program Office's diverse offerings include creating custom thesauri, building customized databases, organizing and publishing research results . . . even providing videos.

For more information about the NASA STI Program Office, see the following:

- Access the NASA STI Program Home Page at ***http://www.sti.nasa.gov***

- E-mail your question via the Internet to help@sti.nasa.gov

- Fax your question to the NASA Access Help Desk at 301–621–0134

- Telephone the NASA Access Help Desk at 301–621–0390

- Write to:
  NASA Access Help Desk
  NASA Center for AeroSpace Information
  7121 Standard Drive
  Hanover, MD 21076

NASA/TM—2003-212589 AIAA–2003–4865

Characterization of Downstream Ion Energy Distributions From a High Current Hollow Cathode in a Ring Cusp Discharge Chamber

John E. Foster and Michael J. Patterson
Glenn Research Center, Cleveland, Ohio

Prepared for the
39th Joint Propulsion Conference and Exhibit
cosponsored by the AIAA, ASME, SAE, and ASEE
Huntsville, Alabama, July 20–23, 2003

National Aeronautics and
Space Administration

Glenn Research Center

October 2003

Available from

NASA Center for Aerospace Information
7121 Standard Drive
Hanover, MD 21076

National Technical Information Service
5285 Port Royal Road
Springfield, VA 22100

Available electronically at http://gltrs.grc.nasa.gov

Characterization of Downstream Ion Energy Distributions From a High Current Hollow Cathode in a Ring Cusp Discharge Chamber

John E. Foster and Michael J. Patterson
National Aeronautics and Space Administration
Glenn Research Center
Cleveland, Ohio 44135

The presence of energetic ions produced by a hollow cathodes operating at high emission currents (>10A) has been documented in the literature. As part of an ongoing effort to uncover the underlying physics of the formation of these ions, ion efflux from a high current hollow cathode operating in an ion thruster discharge chamber was investigated. Using a spherical sector electrostatic energy analyzer located downstream of the discharge cathode, the ion energy distribution over a 0 to 60 eV energy range was measured. The sensitivity of the ion energy distribution function to zenith angle was also assessed at 3 different positions: 0, 15 and 25 degrees. The measurements suggest that the majority of the ion current at the measuring point falls into the analyzer with an energy approximately equal to the discharge voltage. The ion distribution, however, was found to be quite broad. The high energy tail of the distribution function tended to grow with increasing discharge current. Sensitivity of the profiles to flow rate at fixed discharge current was also investigated. A simple model is presented that provides a potential mechanism for the production of ions with energies above the discharge voltage.

Nomenclature

a =Minimum radius of orifice plate channel (m)
e = 1.6 x 10^{-19} C
E_n =Energy acquired after n^{th} bounce (eV)
E_{o1} =Energy of rebounding particle (eV)
E_o =Energy of incident ion (eV)
E = Ion energy (eV)
n_e =Electron number density
l_{cex} =Charge-exchange mean-free path (m)
l_{nn} =Neutral-neutral mean-free path (m)
M_1 =Mass of incident ion (kg)
M_2 =Mass of target material (kg)
N =Minimum number of bounces
n =Bounce index number
d= Distance between ESA and entrance (m)
R =Electrostatic energy analyzer mean radius (m)
r_1 =Radius of inner sector of electrostatic energy analyzer (m)
r_2 =Radius of outer sector of electrostatic energy analyzer (m)
V_p=Plasma potential measured with respect to cathode potential (V)
U= Upper level excited state energy (eV)
ΔE =ESA energy resolution (eV)
ΔV =Potential difference between ESA spherical sectors (V)
ϕ =Sector angle (degrees)
ω =Entrance aperture diameter (m)
α = Ratio of mass of incident ion to mass of target
λ_s =Cathode sheath thickness (m)
V_c =Cathode fall voltage (V)
V_d =Discharge voltage (V)
v_E =Velocity component parallel to cathode sheath electric field (m/s)
v_T =Random thermal velocity (m/s)
θ_{Max} =Maximum rebounding angle (degrees)
L =Channel length
φ =Chamfer angle

Introduction

Deep space missions utilizing ion thrusters will require very long thrusting times.[1,2] Such long operation times place demanding requirements on the lifetime of thruster components. Components such as the ion optics and the discharge and neutralizer hollow cathodes are continuously subjected to erosion processes driven by ion bombardment via either direct impingement or charge exchange.

Hollow cathodes are subjected to ion bombardment from the surrounding discharge plasma. Additionally, as evidence suggests, under certain conditions, cathodes may be a source of very energetic ions that can drive self-erosive processes as well as the erosion of upstream surfaces such as the screen grid. Indeed it was the erosion of internal discharge chamber structures such as the cathode baffle that led to the first suppositions hinting at the existence of an energetic heavy particle beam emanating from the discharge cathode. Studies led by Manteneiks,[3] Rawlin,[4] and Brophy/Garner[5] all observed severe baffle erosion that was suggestive of energetic ion bombardment. Findings from these studies eventually led to the initiation of studies aimed at determining the underlying mechanism for the observed erosion. The bell jar studies of Wilbur[6] determined that there were indeed very energetic ions originating at the discharge hollow cathode. These studies indicated that the magnitude of the energetic ion component increases with increasing discharge current. To date, the production of energetic ions in hollow cathode discharges has been documented by a number of studies.[6–12] Theories attempting to describe the production mechanisms of these ions range from the existence of a potential hill,[6,8,10] to magnetohydrodynamic[7] effects to charge-exchange[9] to hydrodynamic drag driven primarily by electron-ion collisions.[11] Presently, however, there has been no satisfactory complete explanation offered for the production of the energetic ions.

The work presented here represents a continuation of ongoing research aimed at fully characterizing ion emission efflux from a high current hollow cathode.[10] In this present work, the spherical sector electrostatic energy analyzer is used to measure the ion energy distribution as a function of zenith angle relative to the cathode axis as well as discharge cathode flow rate. The study presented here was conducted in a multi-cusp magnetic environment characteristic of ion thruster operation as described in an earlier work.[10] In this respect the findings are likely representative of ion thruster operation in regards to plasma production mechanisms and in particular plasma containment by the axial magnetic field in the near-cathode region.[11]

Experimental set-up

The experiments were conducted in a 91 cm long by 48 cm in diameter cryo-pumped bell jar shown in Figure 1a. The "bell", which was made of Pyrex, allowed for excellent visual inspection of the discharge as illustrated in Figure 1b. The discharge itself was generated using a NASA's Evolutionary Xenon Thruster (NEXT) hollow cathode. A cathode assembly included a coaxial keeper electrode assembly. This electrode was allowed to float during this investigation. The nominal floating potential over the operating range investigated here was approximately 5 V. The hollow cathode was installed in a 30-cm discharge chamber of similar geometry to that of the NASA Solar Electric Propulsion Technology Application Readiness (NSTAR) thruster. Again, the choice of conducting the investigation of energetic ion efflux using a hollow cathode in a ring cusp discharge chamber was made primarily to determine the nature of the ion efflux in a thruster-like environment. The magnetic field near the cathode tip was approximately 90 G. For this study the hollow cathode was operated grounded.

The energy distribution of the ion flux exiting the discharge chamber was characterized using an electrostatic spherical sector energy analyzer (ESA). The ESA was located on axis with the hollow cathode, separated by approximately 23 cm. A schematic of this experimental set-up is illustrated in Figure 2. The analyzer consisted of two spherical sectors (141 degrees in this case) in which the potential of each relative to ground was varied. The potentials on these surfaces determine the energy of which an entering particle must have in order to pass through from entrance slit to exit slit. In this respect, the ESA can be operated as an energy selector. The energy of the particles that can pass through can be calculated based on the geometry and potential difference between the spherical surfaces:

$$E = \frac{\Delta V}{\frac{r_1}{r_2} - \frac{r_2}{r_1}} \tag{1}$$

with an energy resolution also determined by geometry and energy:

$$\frac{\Delta E}{E} \approx \frac{\omega}{R \cdot (1 - \cos\phi) + d \cdot \sin\phi} \tag{2}$$

The ESA was operated in a constant transmission energy mode. A schematic of the electrical connections for operation and data acquisition from the ESA is illustrated in Figure 2b. The transmission energy as determined by the potential difference between the two spherical surfaces was set at 10 eV. With this transmission energy, the energy resolution was approximately 0.347 eV. The input slit varied in potential so that ions with energies between 0 and approximately 60 eV could be scanned. This mode of operation is similar to that used by Kameyama and Wilbur in their investigation of ion efflux from high current hollow cathodes.[8] The ESA was housed in an iron box so as to reduce the effect of the local magnetic field generated by the thruster discharge chamber. The

magnetic field at the entrance slit of the ESA was less than 1 G. In order to minimize the flow of plasma into the device, a cup made of very fine, electro-etched nickel was placed over the entrance slit. The mesh make-up was 20 lines per mm with a 0.039 mm spacing between lines. The nickel wire that made up the mesh was 0.01 mm in diameter. The mesh and the iron box were fixed at ground potential. The electrostatic energy analyzer was suspended over the discharge chamber via a perforated aluminum termination plate. The plate, which located roughly 8.5 cm downstream of the discharge exit plane, contained 8–5.5 cm diameter holes and one 8.5 cm in diameter center hole. This plate was operated at cathode potential during this investigation.

This open geometry was chosen because of its higher conductivity of neutrals away from the discharge chamber as compared to discharge studies with a simulated grid terminating the exit plane. The open geometry of the test apparatus allows the discharge pressure to be maintained at values similar to that of the bell jar. Because the bell jar pressures are similar to those that prevail in ion thrusters (~0.013 Pa ($\sim 1 \cdot 10^{-4}$ Torr)), the discharge characteristics are expected to be similar to actual ion thruster operation, thereby circumventing issues associated with gridded discharge studies.[13] This notion is supported by the magnitude of the discharge voltages measured during the tests (many of which were similar in magnitude to NSTAR engine operation (~26 V).

As indicated in Figure 2b, plasma properties at select location in the discharge chamber was measured using three cylindrical Langmuir probes. The collecting surface of each probe was made of tungsten wire. Two of the probes were located in a plane normal to the discharge axis but located a ~3 mm downstream of the cathode keeper. These probes, whose tips were 0.38 mm in diameter and 3 mm long were used to assess plasma properties in the plane which approximately contained the face of the keeper. One probe was located approximately 2 mm off-axis. The second of the keeper plane probes was located approximately 2 cm above the surface of the anode. In this regard, the probes could be used to determine the average potential difference between these two points. A third probe, 5.5 mm long, 0.38 mm in diameter was used to measure plasma properties near the entrance slit of the ESA. This probe was located approximately 2 cm below the energy analyzer and approximately 1 cm off-axis of the energy analyzer.

Experimental Results and Discussion

The ion energy distribution was measured as a function of both discharge current at a fixed flow rate and as a function of flow-rate at fixed discharge current. For all operating conditions, the bell jar pressure never exceeded 1.5×10^{-4} Torr. Ion energy spectra were collected over a wide discharge current range (8–16 A). Before plasma measurements were taken, the discharge was allowed to stabilize at each operating condition. In all cases, the peak-to-peak oscillations in the discharge voltage were less than 3 volts.

Figure 3 shows typical variations in discharge voltage at a fixed flow rate as a function of discharge current over an extended range. The discharge voltage increases linearly with increasing discharge current up to nearly 16 A, at which point the discharge voltage appears to plateau.

Ion Energy Distribution Measurements

One primary objective of this work was to investigate the possible existence of energetic ions emitted from the hollow cathode. Energetic ion flux produced at or near the discharge cathode should be detectable by the downstream located ESA. The energy range of the investigation was extended to approximately 60 eV. Energies above 60 eV were not investigated as it was found that at ESA entrance slit bias voltages required to measure this energy range perturbed the plasma. Measurements made at Colorado State University suggest that there is an angular dependence to the ion energy distribution function. Indeed, findings from the group indicates that the energetic ions are detectable off-cathode axis.[14] In order to determine if such phenomena prevails with the 1.27 cm NEXT discharge cathode, ion energy distribution functions where characterized as a function of zenith angle relative to the axis of the discharge cathode.

ESA Zenith Angle = 0 degrees

Figure 4 shows the variations in the of the ion energy distribution function as at a discharge current of 13.6 A As the flow rate is reduced from 4.3 SCCM to 3 SCCM. As can be seen in the Figure, the peaks are fairly broad and centered near an energy roughly commensurate with the discharge voltage. The location of the central peak was on average approximately 5 eV below that which would be expected of an ion falling through a sheath potential difference comparable to the discharge voltage. This observation is consistent with similar measurements made elsewhere.[8,12] Part of the discrepancy is due to the absolute uncertainty in the discharge voltage whose peak to peak variations were as much as 1–2 V . The remaining energy discrepancy could be attributed to ions born near the analyzer on a potential plateau that is lower than the plasma potential in the bulk discharge. Langmuir probe measurements made near the analyzer appear to support this notion. The plasma potential

measurements made near the analyzer were consistently lower than the discharge voltage by approximately 3–10 V. Figure 5 illustrates the difference between the plasma potential as measured just downstream of the energy analyzer and the discharge voltage for a number of different discharge currents at 4.3 SCCM.

The broad peaks observed were distributed over a fairly large energy range, with the leading edge and trailing edge expanding into higher energies with increasing flow rate. The variation in the full width half maximum (FWHM) increased linearly with increasing flow rate changing from just of 8 eV at 3.5 SCCM to over 13 eV at 4.3 SCCM. This behavior with increasing flow rate (cathode pressure) is attributed to an increase in scattering events. In this regard, it can be characterized as a form of collisional broadening. Such broadening increases the energy distribution counts on both low energy and higher energy sides of the peak. At fixed discharge current, the peak intensity also increases with increasing flow rate. The nearly linear increases in peak height with increasing flow rate is consistent with observed increases in plasma density measured just upstream of the analyzer.

The absolute peak width, as evaluated at the peak baseline, is somewhat puzzling. The fraction of ions making up the distribution function with energies less than the discharge voltage is attributable to charge exchange ions formed in the region between the analyzer and mesh. This observation is also consistent with similar measurements.[8] On the other hand, the ions with energies well above the discharge voltage potential is not so readily explainable. Though the peaks tended to be centered near energies associated with the discharge voltage, the distribution functions tended to extend 20-30 eV beyond this peak energy. Indeed, at 4.3 SCCM, the wing of the ion energy distribution extended to nearly 60 eV.

As discussed earlier, the peaks tended to narrow and sharpen with decreasing flow rate. Figure 6 illustrates the behavior of the energy distributions at the reduced xenon flow rate of approximately 2 SCCM as a function of discharge current. The sharpening of the peaks and particularly the reduction in distribution intensity at the lower energies are likely associated with reduced collisional broadening. In all cases the location of the distributions' peaks tended to track changes in the discharge voltage. Also, as can be seen in Figure 6, there is a noticeably sharp rise in intensity on the low energy side of the distributions. In fact, the sharp rise in intensity occurs at nearly the same energy, just over 22 eV , for all the plots acquired at this fixed flow rate. This sharp rise is indicative of magnitude of the potential drop that that exists between the mesh that covers the analyzer and local plasma potential. Indeed, this value of 22 eV is consistent with the plasma potential measurements made just downstream of the analyzer whose average value for these operating conditions was approximately 23.5 V.

With increasing discharge current, the absolute width of the distribution broadened, extending to higher energies—to nearly 25 eV above the discharge voltage! The FWHM increased linearly with increasing discharge current, increasing from approximately 5 eV at 13.3 A to nearly 8 eV at 15.6 A. These expansion towards higher energies in the distribution function tail indicate that the population of energetic ions increase with increasing discharge current. The ion signal at all energies increased with increasing discharge current. Indeed, the peak intensity increased linearly with increasing discharge current. This behavior over this limited current range is associated with the measured increases in the plasma density. It is interesting to note, however, that the population of ions in the tail grows much more rapidly than those at the peak. For example, the ion signal at 33 eV increases exponentially with increasing discharge current. This finding suggests different origins for ions in the tail as opposed to those near the most probable value. The energy distributions taken at fixed currents and fixed flow-rates all indicated the presence of energetic ions-with energies well in excess of the discharge voltage.

ESA Zenith Angle = 15 degrees

The angular position of the electrostatic energy analyzer was varied using precision machined wedges as illustrated in Figure 7. Ion energy distribution functions taken at different operating conditions at an orientation of 15 degrees are shown in Figure 8. In general, peak intensities at off-axis angles were weaker. This is largely attributed to the fact that to obtain the desired angle the probe also had to be translated radially, in addition to canting the analyzer with respect to its input lens axis. Because the discharge is known to be non-uniform (as inferred from beam current density profiles), the plasma density in the region off axis is lower.[15] The fact that the relative peak intensities were reduced at off axis locations suggests that predominantly, the ions falling into the analyzer are primarily from the discharge and are not a well structured beam propagating from the discharge cathode. As can be seen in the figure, a peak centered near the discharge voltage, which is consistent with the 0 degree orientation cases, again defines the distribution. Additionally, as observed in the 0 degree case, the distributions tended to expand to higher energies with increasing discharge current. The low energy "shoulder" extended to significantly lower energies than in the 0 degree orientation case. This new feature became more pronounced with increasing angle. The presence of the low energy shoulder is most likely due to a combination of charge exchange, scattering

within the analyzer, sheath uniformity (or lack thereof) at the analyzer mesh cover, and orientation of the analyzer, which examines the component of the ion falling out of the plasma that is parallel to the analyzer axis itself. It should be pointed out that at this orientation, the wings of the ion energy distributions indicate overpopulation relative to what would be expected on a Gaussian distribution, suggesting superthermal ions.

ESA Zenith Angle =25 degrees

Examination of spectra taken at a zenith angle of 25 degrees possessed additional structure on the low energy side of the ion distribution but no additional structure was observed on the high energy side. As in the 0 and 15 degree case, a primary peak was observed centered near the discharge voltage. These profiles also extended to energies well above the discharge voltage, as indicated in Figure 9. The presence of distinct peaks other than the central peak, however, was not observed. A more pronounced low energy "shoulder" was also observed.

In general, these findings differ from those taken at CSU in that over the energy range investigated, the presence of distinct, high energetic ion beams emanating from the cathode region were not observed.[14] This is not to say that energetic ions were not measured. Indeed, as mentioned earlier in each case, ion signals associated with energies well above the discharge voltage were observed. This signal is associated with ions that may be emanating from the cathode as suggested by other work.[14] Presumably, these ions have not significantly equilibrated with the background ion population. In this work the energetic ions appeared as overpopulated wings of the distribution function. In this respect the ion current distribution may be characterized best as a Gaussian with a superthermal tail that increases in magnitude with increasing discharge current. The differences initially were attributed to the fact that the early CSU experiments were performed in configurations dissimilar for an ion thruster discharge chamber.[6] Recent results however indicate that this may not be the case. A more likely reason for the difference may be found in the very nature of the hollow cathode itself. The orifice size of the GRC cathode and the CSU cathode differ significantly. For example, the GRC orifice diameter is nearly twice that of the CSU cathode. As a result, at a given flow rate, internal pressures inside the cathodes are markedly different. The differences in internal pressure environments can effect the distribution function directly as will be discussed in the next section.

Potential Mechanism for the formation of energetic ions in a hollow cathode discharge

In general, findings from this work differ from those taken at CSU in that over the energy range investigated, the presence of distinct, high energetic ion beams emanating from the cathode region were not observed.[14] This is not to say that energetic ions were not measured. Indeed, as mentioned earlier in each case, ion signals associated with energies well above the discharge voltage were observed. This signal is associated with ions that may be emanating from the cathode as suggested by other work.[6,14] In this work, the energetic ions appeared in the wings of the distribution function. In this respect, the ion current distribution may be characterized best as a Gaussian whose tail population increased in magnitude with increasing discharge current. The differences initially were attributed to the fact that the early CSU experiments were performed in configurations dissimilar from an ion thruster discharge chamber.[6] Recent results however indicate that this may not be the case. A more likely reason for the difference may be found in the very nature of the hollow cathode itself. The orifice size of the GRC cathode and the CSU cathode differ significantly. For example, the GRC orifice diameter is nearly twice that of the CSU cathode. As a result, at a given flow rate, internal pressures inside the cathodes are markedly different.

Internal cathode number densities determine the governing collisional processes that take place there. A potential mechanism based on collisions taking place inside the cathode is proposed for formation of energetic ions observed in other work. This proposed model is based on an energy gain process that depends on collisions taking place within the orifice channel of the discharge cathode.

Ions produced within the hollow cathode discharge that have velocities directed toward cathode surfaces (barring scattering events) enter the cathode sheath. There the ion accelerates toward the cathode surface, ultimately attaining an impact energy proportional to the cathode fall voltage: $e \cdot V_c$. The ion upon collision with the cathode surface is usually neutralized. A fraction of the ion's incident kinetic energy is converted to thermal energy which contributes to the maintenance of the cathode temperature. The remaining energy resides as kinetic energy of the rebounding ion or neutral. The fraction of the incident energy that the neutralized ion rebounds with can be described by the following relation:[16–19]

$$\frac{E_1}{E_{o1}} = \left(\frac{\cos(\theta) + \sqrt{(M_2/M_1)^2 - (\sin(\theta))^2}}{1 + M_2/M_1} \right)^2 \qquad (3)$$

This relation is derived based on binary collision physics in which momentum and energy are conserved. A schematic of scattering interaction is shown in Figure 10. According to equation 3, the energy of the scattered particle decreases with increasing angle. Scattered particles with angles nearly parallel to the hollow cathode orifice channel wall rebound with the largest fraction of the incident energy. For normal incidence and specular reflection (incidence angle equals reflection angle), the scattering angle θ is 180. Equation 3 then reduces to

$$\frac{E_{o1}}{E_o} = \left(\frac{\alpha - 1}{\alpha + 1} \right) \qquad (3')$$

where

$$\alpha = M_2 / M_1 \qquad (4)$$

The fraction of incident energy that rebounding particle leaves the surface increases with α.

Assuming a 180 degree scattering angle (Equation 3'), in the case of xenon plasma within a hollow cathode, incident ions impinging upon the tungsten insert or tungsten orifice plate gives rise to an α that is approximately 1.4. It then follows from Equation (3') that approximately 17 percent of the incident ion energy leaves as kinetic energy with the neutral; that is, a 25 eV ion, for example, incident on the cathode leaves the cathode surface as a 4.25 eV neutral.

Energetic ions can be generated in the cathode if the ion undergoes multiple impacts with cathode surfaces n-times before exiting the cathode. This energy gain mechanism relies on charge-exchange events taking place inside the hollow cathode. Figure 11 illustrates an exaggerated view of the mechanics of the energy gain process. Here, an ion incident upon the cathode surface leaves the surface as a low energy neutral. The neutral then proceeds to the opposite cathode surface. Before it reaches the sheath, it undergoes either a charge-exchange collision or an electron impact ionization event where it becomes a low energy ion still directed to the cathode surface. The particle then accelerates again only to rebound from the surface as a neutral once again. However, the resulting neutral is slightly more energetic because the incident ion was also slightly more energetic because of its additional energy from the first impact. The process then repeats itself but is directed at the opposite orifice channel wall. Repeated impacts of this nature give rise to an energy accumulation process in which the ion can exit the cathode at energies greater than the cathode sheath potential. The exit energy of a given ion depends on where the energy gain process began in the orifice channel. This tends to broaden the ion energy spectrum of exiting ions, thereby contributing not only to the spread in ion energy but also contributing to the population of the high energy tail. It should be pointed out that this process could give rise to the cathode emission of both energetic ions and neutrals. In the case of the neutrals, the energetic neutral escapes out of the orifice before a charge-exchange collision can take place. These processes could potentially lead to cathode orifice erosion as well provided the particles' kinetic energy exceed the sputtering threshold.[20]

This process of energy gain depends on a number of length scales. Indeed, if the length scales do not satisfy certain conditions, the energy gain process will not be resonant and thus the fraction of energetic neutrals and ions generated cannot be expected to be appreciable. The length scales of particular importance include the 1) cathode orifice channel diameter, 2) electron-neutral ionization path-length, 3) ion-neutral resonant charge-exchange path-length, 4) neutral-neutral collision mean free path, and 5) cathode sheath thickness. Whether or not these energetic particles form by this mechanism requires that the inequality:

$$\lambda_s < l_{cex} \approx l_i < a < l_{nn} \qquad (5)$$

be satisfied. In this respect, this energy gain process is favored if conditions of low pressure and high orifice ionization fractions prevail. For cathode neutral pressures of interest, because the neutral-neutral mean free path is less than the cathode insert inner diameter, in contrast to the orifice, energy gain processes taking place inside the insert are not expected to be significant.

The energy gain per impact can be determined analytically if specular reflection is assumed. Here, equation 3' applies and thus the energy that an ion or neutral can gain during the impacting process increases arithmetically with impact number. The energy of the particle after the n^{th} impact can be determined:

$$E_n = [1 + \gamma \cdot (n-1)] \cdot V_c \cdot \gamma \qquad (9)$$

where γ corresponds to the energy attenuation factor defined by the right-hand side of Equation 3'. This factor depends only on mass ratio. The energy gained by a xenon particle as a function of number of impacts (bounces) within in the orifice channel is illustrated in Figure 12. Baring any collisions besides charge exchange, the xenon particle will oscillate radially between wall surfaces within a plane whose normal is

nearly parallel with the axis of the channel. In doing so, with each impact, the particle's energy would increase. Surface texture of the channel, collisions with the particles that make up the ionized gas within the channel, potential gradients, as well as drift due to small but finite non-radial velocity components associated with the thermal energy of the particle ultimately causes the oscillating particle to "random walk" toward the exit planes of the channel (See Figure 11). The particle trajectory itself may be roughly thought of as a helix as it bounces from side to side traveling along the axis of the cathode toward the channel exit planes.

If it is assumed that the cathode sheath voltage is 17 V, the particle can easily obtain an energy equivalent to the cathode fall voltage provided the channel length is greater than 1 mm. [21]

Conclusions

Low energy ion spectra were acquired at three different zenith angles to characterize the ion emission from a NEXT discharge hollow cathode inside a discharge chamber. Ion spectra appearance were best characterized as broad peaks that tended to extend toward higher energies with increasing discharge current. The distribution functions tended to spread in energy on both the low energy and high energy side with increasing flow rate. The data indicate that the dominant ion signal is due to discharge ions falling out of the discharge plasma. Energetic ions were detected only in the tail of the distribution function.

A mechanism for generating energetic ions was proposed. Energetic ions can be produced by resonant collisions taking place inside the orifice channel. An ion can be generated with appreciable energies due to multiple impacts between cathode surfaces. The conditions that allow such a process to take place depend on key mean free paths (electron-neutral, neutral-neutral, resonant charge-exchange) relative to the characteristic length-scale of the orifice channel and orifice channel ionization fraction. Though a conservative estimate of the energy of the exiting ions can be determined, Monte Carlo or similar computational techniques are necessary to elucidate the details of the phenomenological model. The model presented here points to internal hollow cathode processes that could be exploited in the form of a low energy ion source. Experimental validation of this model is left to a future investigation.

References

[1]Shotwell, R., " Carbon-Carbon Grid Development for Ion Propulsion Systems," IEPC Paper 2001-093, October 2001.

[2]Rawlin, V.K. et al, "High Specific Impulse, High Power Ion Engine Operation," AIAA Paper 2002-3838, July 2002.

[3]Mantenieks, M.A. and Rawlin, V.K., "Studies of Internal Sputtering in a 30-cm Ion Thruster," 11th Electric Propulsion Conference, New Orleans, Louisiana, March 19-21, 1975.

[4]Rawlin, V.K., "Internal Erosion Rates of a 10-kW Xenon Ion Thruster," AIAA Paper 88-2913, 24th Joint Propulsion Conference, Boston, Massachusetts, July 11-13, 1988.

[5]Brophy, J.R. and Garner, C.E., "Tests of High Current Hollow Cathodes for Ion Engines," AIAA Paper 88-2913, 24th Joint Propulsion Conference, Boston, Massachusetts, July 11-13, 1988.

[6]Friedly, V.J. and Wilbur, P.J., "High Current Hollow Cathode Phenomena," *Journal of Propulsion and Power*, Vol. 8, No. 3, May-June, 1992, pp. 635-643.

[7]Latham, P.M., Pearce, A.J., and Bond, R.A., "Erosion Processes in the UK-25 Ion Thruster," IEPC Paper 91-096, 22nd International Electric Propulsion Conference, Viareggio, Italy, October 14-17, 1991.

[8]Kameyama, Ikuya and Wilbur, P.J., "Measurements of Ions from High Current Hollow Cathodes Using Electrostatic Energy Analyzer*," Journal of Propulsion and Power*, Vol. 16, No. 3, May-June 2000, pp. 529-535.

[9]Crofton, M.W., "The Feasibility of Hollow Cathode Ion Thrusters: A Preliminary Characterization ,"AIAA Paper 2000-5354, July 2000.

[10]Davis, W.D., and Miller, H.C., "Analysis of the products emitted by dc arcs in a vacuum ambient*," J. Appl. Phys*, Vol. 40, pp. 2212-2221, 1969.

[11]Hantzsche, E., "A Hydrodynamic Model of Vacuum Arc Plasma," *IEEE Transactions on Plasma Science*, Vol. 20, No. 1, February 1992.

[12] Foster, J.E. and Patterson, M.J., Plasma emission characteristics from a high current hollow cathode in an ion thruster discharge chamber," AIAA Paper 2002-24102, Indianapolis, 2002.

[13]Brophy, J.R., "Simulated Ion Thruster Operation without Beam Extraction," AIAA, DGLR, and JSASS 21st International Electric Propulsion Conference, Orlando, FL, 1990, AIAA Paper 90-2655.

[14] Farnell, C.C., Williams, J.D., and Wilbur, P.J., "Characteristics of Energetic Ions Emitted from Hollow Cathodes," Proceedings of the 28th International Electric Propulsion Conference, IEPC paper 03-072, Toulouse, France, 2003.
[15]Foster, J.E., Soulas, G.C., and Patterson, M.J., "Plume and Discharge Plasma Measurements of an NSTAR-type Ion Thruster," AIAA Paper 2000-3812, Huntsville, 2000.
[16]Smith, D.P., "Scattering of Low-Energy Nobel Gas Ions From Metal Surfaces," *Journal of Applied Physics*, Vol. 38, No. 1, Jan. 1967, pp. 340-347.
[17]Goff, R.F. and Smith, D.P., "Surface Composition Analysis by Binary Scattering of Noble Gas Ions," *The Journal of Vacuum Science and Technology*, Vol. 7, No. 1, 1967, pp. 72-75.
[18]Brongersma, H.H. and Mul, P.M., "Ion Scattering: A Spectroscopic Tool For Study Of the Outermost Atomic Layer Of A Solid Surface," *Chemical Physics Letters*, Vol. 14, No. 3, June 1972, pp. 380-384.
[19]Fauster, Th, "Surface geometry determination by large-angle ion scattering," *Vacuum*, Vol. 38, No. 2, 1988, pp. 129-142.
[20]Williams, G.J., et al, "FMT-2 Discharge Cathode Erosion Rate Measurements via LIF," AIAA Paper 2000-3663.
[21]Salhi, A., Myers, R.M., Turchi, P.J., "Experimental Investigation of a Hollow Cathode Discharge, IEPC Paper 93-025, Sept. 1993.

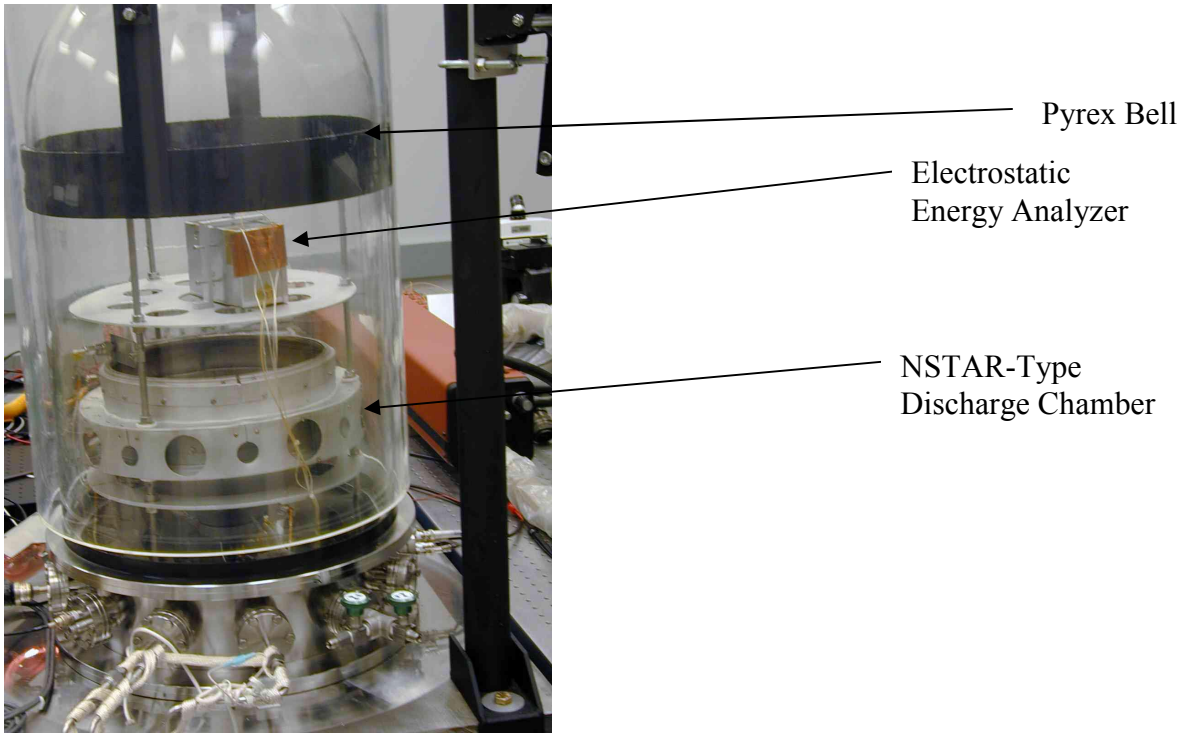

Figure 1a. Bell jar used in this investigation. Note position of discharge chamber and electrostatic energy analyzer.

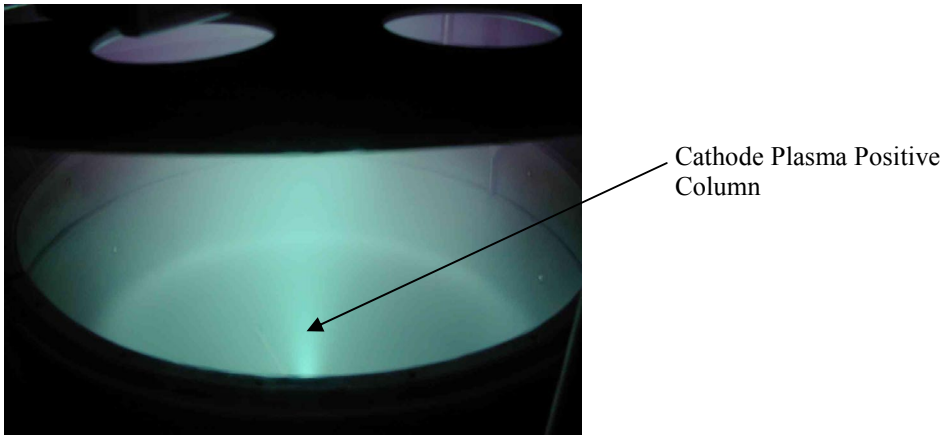

Figure 1b. Discharge operation: Notice cathode plasma (plume emanating from discharge cathode) and main discharge plasma, which appears more diffuse and weaker in intensity.

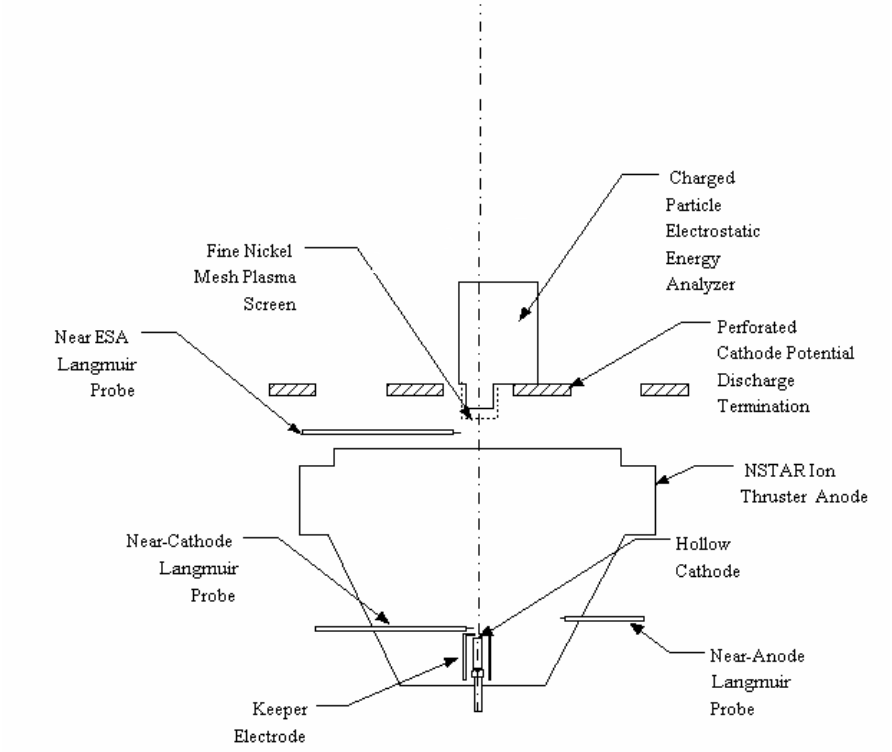

Figure 2a. Pictorial representation of the experimental set-up (not to scale).

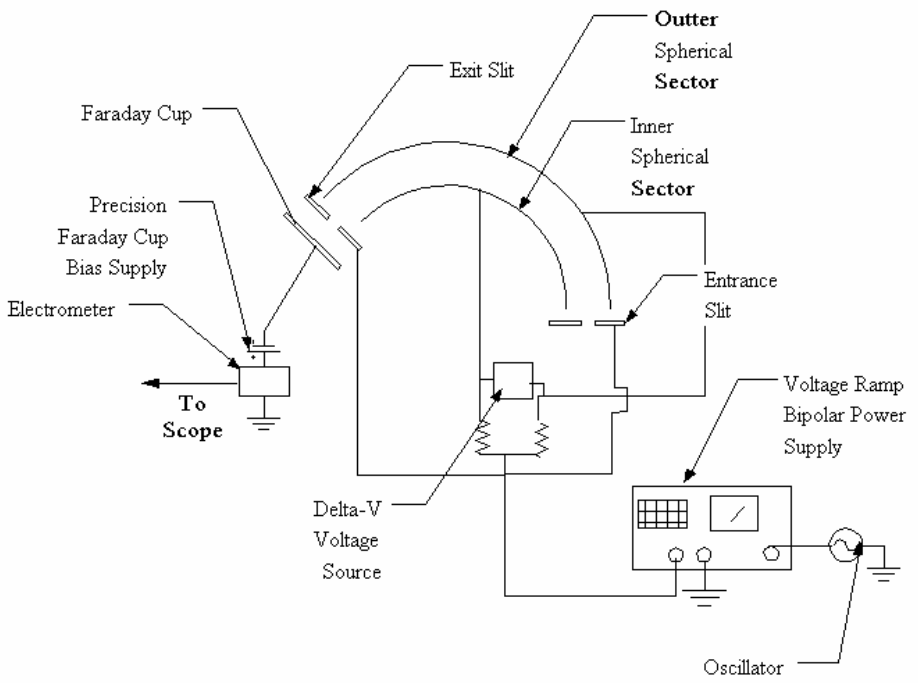

Figure 2b. Electrostatic energy analyzer electrical circuit layout depicting bias supplies and data acquisition.

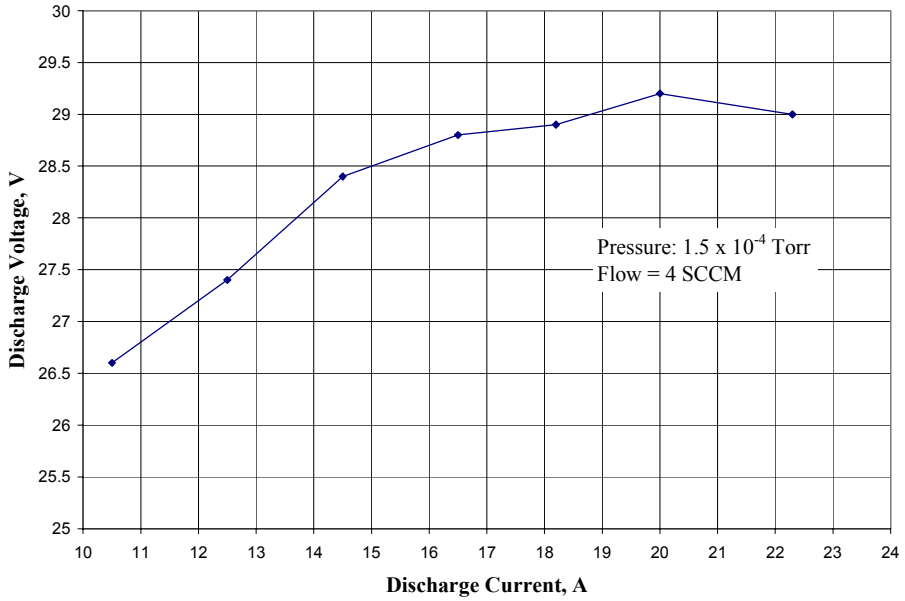

Figure 3. Discharge characteristics of cathode inside NSTAR discharge chamber at fixed flow rate.

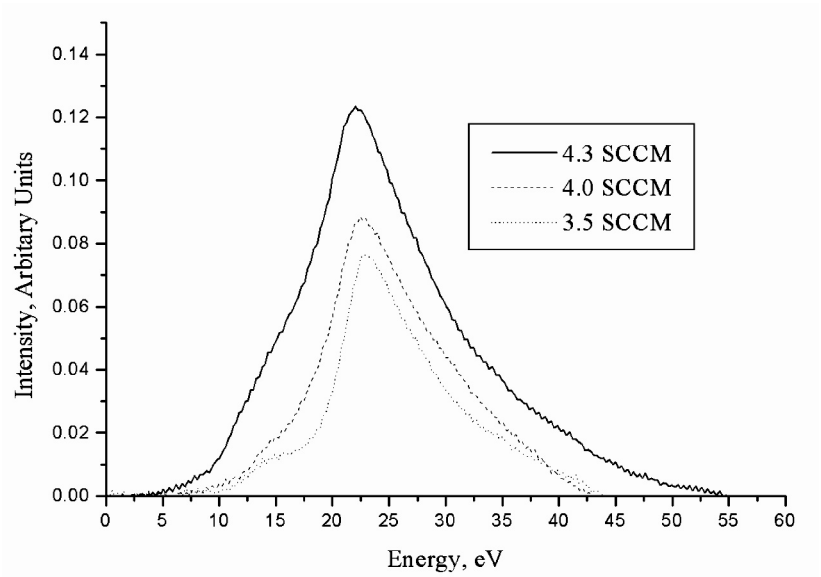

Figure 4. Variations in the ion energy distribution function with flow rate at fixed discharge current: I=13.6 A. Zenith angle = 0 degrees.

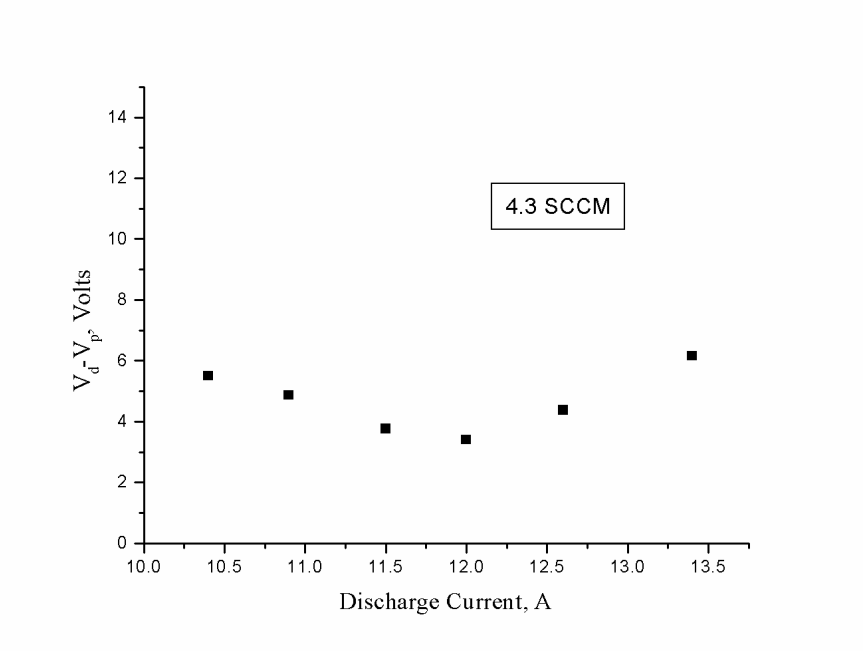

Figure 5. Variations in the difference between peak energy and the potential energy of an ion located just downstream of the analyzer.

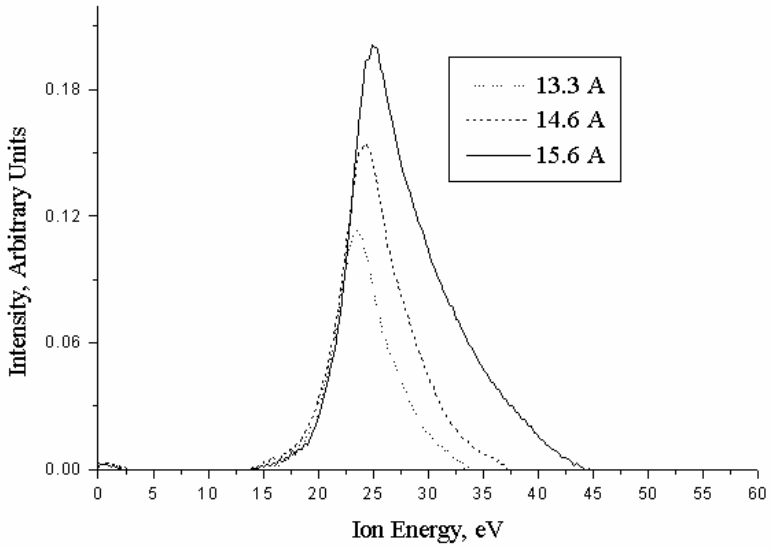

Figure 6 Variation in the ion energy distribution with discharge current at fixed flow: 2 SCCM. Zenith angle = 0 degrees.

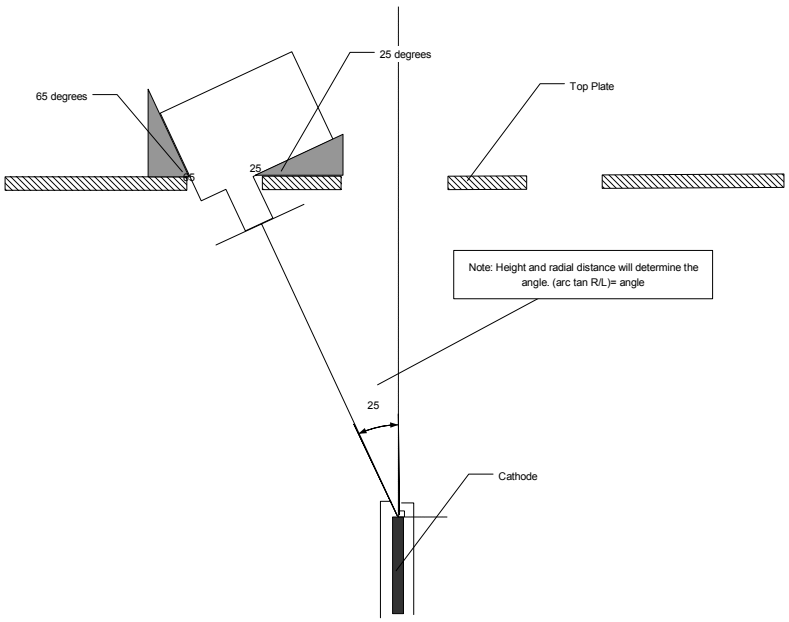

Figure 7. Use of precision machined wedges to vary angular position of the ESA. Case for 25 degree wedges illustrated.

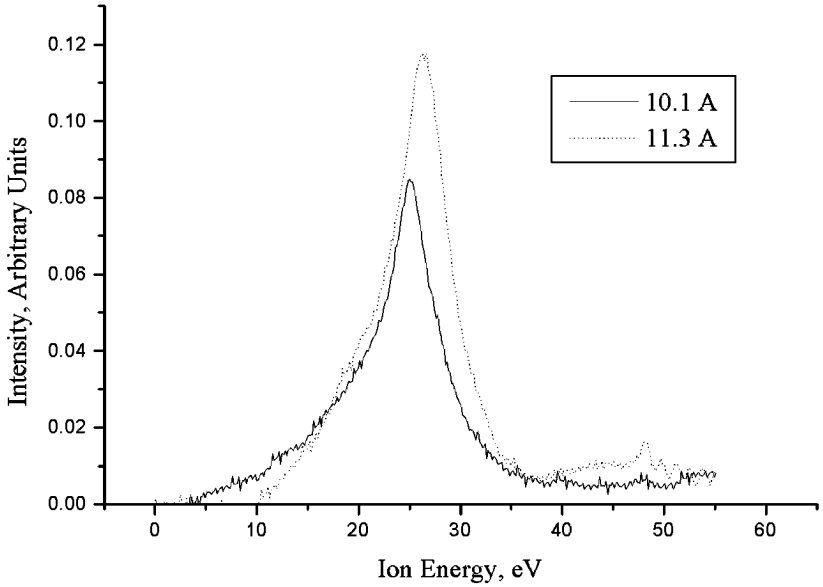

Figure 8. Variation in the ion energy distribution function with discharge current: zenith angle = 15 degrees. Flow = 2 SCCM.

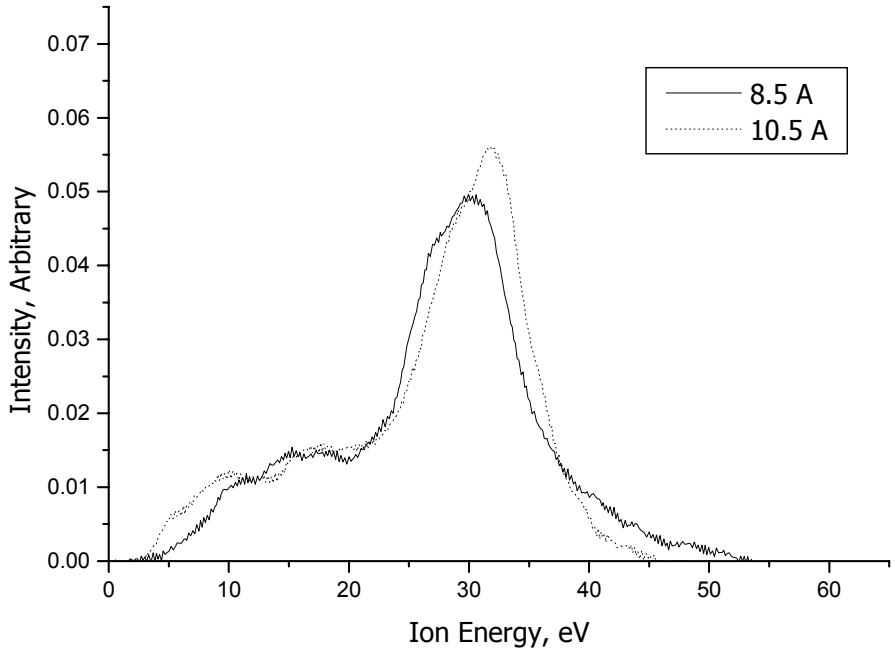

Figure 9. Variation in the ion energy distribution function with discharge current: zenith angle = 25 degrees. Flow =1.9 SCCM.

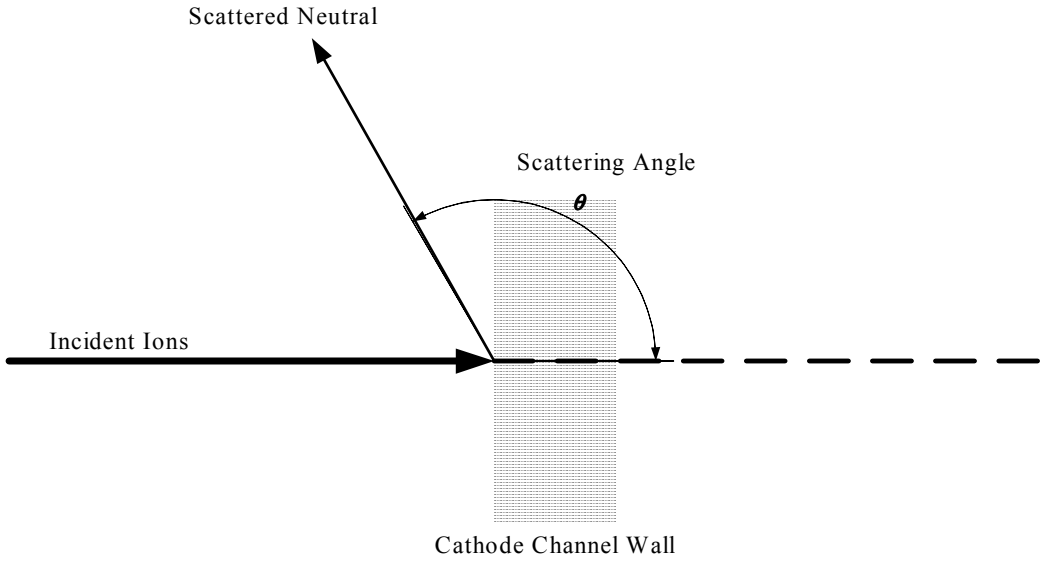

Figure10. Schematic diagram illustrating relevant scattering geometry used in the model.

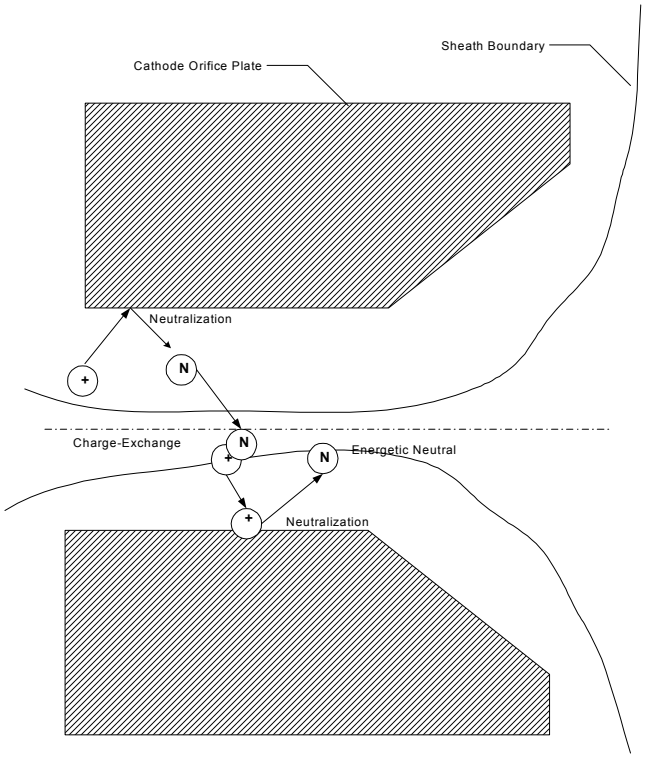

Figure 11. Schematic representation of energy gain process in cathode orifice channel.

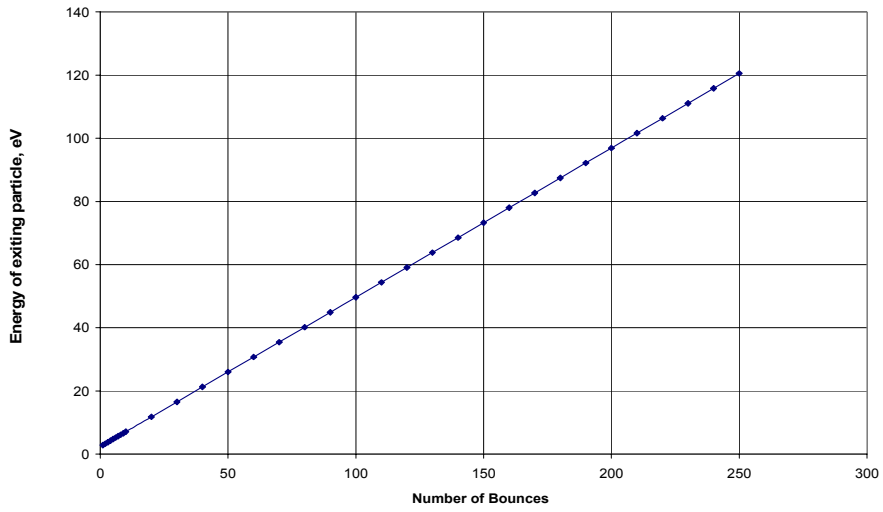

Figure 12. Variation in energy gain with bounce number. Bounce number increases with increasing orifice channel length.

REPORT DOCUMENTATION PAGE

Form Approved
OMB No. 0704-0188

1. AGENCY USE ONLY (*Leave blank*)	2. REPORT DATE	3. REPORT TYPE AND DATES COVERED
	October 2003	Technical Memorandum

4. TITLE AND SUBTITLE

Characterization of Downstream Ion Energy Distributions From a High Current Hollow Cathode in a Ring Cusp Discharge Chamber

5. FUNDING NUMBERS

WBS–22–755–70–04

6. AUTHOR(S)

John E. Foster and Michael J. Patterson

7. PERFORMING ORGANIZATION NAME(S) AND ADDRESS(ES)

National Aeronautics and Space Administration
John H. Glenn Research Center at Lewis Field
Cleveland, Ohio 44135–3191

8. PERFORMING ORGANIZATION REPORT NUMBER

E–14146

9. SPONSORING/MONITORING AGENCY NAME(S) AND ADDRESS(ES)

National Aeronautics and Space Administration
Washington, DC 20546–0001

10. SPONSORING/MONITORING AGENCY REPORT NUMBER

NASA TM—2003-212589
AIAA–2003–4865

11. SUPPLEMENTARY NOTES

Prepared for the 39th Joint Propulsion Conference and Exhibit cosponsored by the AIAA, ASME, SAE, and ASEE, Huntsville, Alabama, July 20–23, 2003. Responsible person, John E. Foster, organization code 5430, 216–433–6131.

12a. DISTRIBUTION/AVAILABILITY STATEMENT

Unclassified - Unlimited
Subject Categories: 20 and 75 Distribution: Nonstandard

Available electronically at http://gltrs.grc.nasa.gov

This publication is available from the NASA Center for AeroSpace Information, 301–621–0390.

12b. DISTRIBUTION CODE

13. ABSTRACT ***(Maximum 200 words)***

The presence of energetic ions produced by a hollow cathodes operating at high emission currents (>10A) has been documented in the literature. As part of an ongoing effort to uncover the underlying physics of the formation of these ions, ion efflux from a high current hollow cathode operating in an ion thruster discharge chamber was investigated. Using a spherical sector electrostatic energy analyzer located downstream of the discharge cathode, the ion energy distribution over a 0 to 60 eV energy range was measured. The sensitivity of the ion energy distribution function to zenith angle was also assessed at 3 different positions: 0, 15, and 25 degrees. The measurements suggest that the majority of the ion current at the measuring point falls into the analyzer with an energy approximately equal to the discharge voltage. The ion distribution, however, was found to be quite broad. The high energy tail of the distribution function tended to grow with increasing discharge current. Sensitivity of the profiles to flow rate at fixed discharge current was also investigated. A simple model is presented that provides a potential mechanism for the production of ions with energies above the discharge voltage

14. SUBJECT TERMS

Hollow cathode; Energetic ions; Plasma; Erosion; Ion thruster

15. NUMBER OF PAGES

21

16. PRICE CODE

17. SECURITY CLASSIFICATION OF REPORT	18. SECURITY CLASSIFICATION OF THIS PAGE	19. SECURITY CLASSIFICATION OF ABSTRACT	20. LIMITATION OF ABSTRACT
Unclassified	Unclassified	Unclassified	